



GSJ: Volume 8, Issue 1, January 2020, Online: ISSN 2320-9186

[www.globalscientificjournal.com](http://www.globalscientificjournal.com)

**INVESTIGATION OF THE EFFECTS OF LEACHATE FROM SOLID WASTE DUMPSITE ON  
GROUNDWATER USING ELECTRICAL RESISTIVITY METHOD.**

**AGADA LIVINUS<sup>1</sup>, ADETOLA S. ONIKU<sup>2</sup>, OSITA MELUDU<sup>2</sup>**

1. Faculty of Science, Yobe State University Damaturu, P.M.B 1144, Damaturu.
2. School of Pure and Applied Sciences, Modibbo Adama University of Technology, Yola.

Correspondence Author: agadaman1908@gmail.com

**ABSTRACT**



This study was carried out to investigate the effects of leachate on groundwater in Gashua, Nigeria. A total of ten (10) vertical electrical resistivity sounding (VES) using Schlumberger electrode configuration and ten (10) profiles of electrical resistivity tomography (ERT) using Wenner electrode configuration were used to investigate the effects of leachate on groundwater in Gashua and its environs. The electrical resistivity field data were interpreted by using Winresist for VES and RES2DINV for ERT. The results of the electrical resistivity survey revealed that the study area is composed of five geoelectrical layers which are; the topsoil, clay, sand, sandy clay and sand. The resistivity of the first layer range from 42.7 to 199.7 $\Omega$ m and its thickness range from 0.6 to 1.9m, the second layer has resistivity ranging from 16.5 to 37.9 $\Omega$ m with a thickness ranging from 4.1 to 10.7m. The resistivity of the third layer ranges from 101.2 to 288.2 $\Omega$ m and its thickness ranges from 38.9 to 99.7m, it is the first aquifer in the study area. The fourth layer has resistivity ranging from 100.7 to 214.3 $\Omega$ m and its thickness ranges from 28.5 to 94m. The fifth layer is the second aquifer and its resistivity ranges from 254 to 350 $\Omega$ m. It has a very large thickness. The aquifer resistivity ranged from 101.2 to 288.2 $\Omega$ m for the first aquifer and from 253.8 to 350.1 $\Omega$ m for the second aquifer. The 2D electrical resistivity tomography (ERT) profiles showed areas of low resistivity zones which were interpreted as zones infiltrated by contaminants from the dumpsites and high resistivity zones depict areas with less or non-conductive materials in the study area. Results from the four solid waste dumpsites showed that leachate from the waste dumpsites infiltrated into the aquifers and polluted the groundwater. The presence of the contaminants in the groundwater was identified by a decrease in the formation resistivity values. It is evident, from the results of the geophysical survey that the water in the study area is polluted and it is responsible for the prevalence of water related diseases common in the study area.

Keywords: Resistivity, leachate, groundwater, pollution, geophysical and infiltration.

## **INTRODUCTION**

Groundwater is the major source of drinking water in the semi-arid region of Nigeria. Its quality is mostly compromised in towns and cities due to increased human activities which has led to the production of large tons of solid waste materials daily, and they are poorly disposed. Municipal solid waste contains hazardous constituents, such as volatile organic compounds and heavy metals. A leachate is any liquid that, in the course of passing through matter, extracts soluble or suspended solids, or any other component of the material through which it has

passed. Leachate released into groundwater may cause severe risks to human health and the environment. Groundwater pollution due to leachate infiltration into the subsurface has been on the rise in recent times, due to the production of large amount of solid waste through domestic, agriculture and industrial processes. The release of leachate into the subsurface may render groundwater unfit for drinking and other uses. Leachate released into groundwater may also cause danger to the environment by enhancing the growth of toxic substances. Leachate from solid waste disposal sites mostly contains chemical elements such as calcium, potassium, mercury, copper, iron, manganese, chromium, nickel, lead, nitrogen, ammonia, acetone, benzene, toluene, chloroform, selenium, cyanide, arsenic, cadmium, etc. (Freeze and Cherry, 1979). These chemical substances in their elevated concentrations in groundwater and soil can cause kidney disease, lung damage, liver and bladder complications, nausea, cancer and vomiting, etc. (ATSDR, 2000). There were reports of suspected cases of health complications associated with drinking of contaminated water in Gashua and its environs.

Large amount of solid waste generated daily from domestic, industrial and agricultural activities are not properly disposed. Most of the wastes are dropped openly at the dumping sites. The leachate generated by these waste materials always goes into the subsurface to pollute the groundwater. In recent times, the impact of leachate on both ground and surface water has attracted the attention of many researchers. Amidu et al., (2006); Oladunjoye et al., (2011); Olayinka and Olayinwola (2001), have used electrical resistivity imaging to delineate contaminant transport from leachate in a basement complex terrain. Pollution of groundwater happens due to the percolation of fluvial water and infiltration of contaminants through the soil in waste disposal sites (Abdullahi et al., 2011). Leachate is a liquid formed from the decomposition of waste and has high conductivity due to the presence of dissolved salts. The electrical resistivity of leachate is often very much lower than natural groundwater. Pollutants or contaminants released into the environment rarely remains at the point of discharge. They are transported through the porous soil by the process of adsorption, advection, molecular diffusion and dispersion. Leachate is generally associated with high ion concentrations and therefore rock formation containing them is characterized with very low resistivity (Cristina et al., 2012). This makes electrical resistivity techniques most adequate for mapping the extent of leachate contamination around landfills (Bernstone et al., 1999).

Keller and Frichescht(1999) used 2D electrical resistivity imaging and vertical electrical sounding to estimate the depth to the groundwater table, identify and delineate the extent of contaminant plume and migration path below surface around landfill. Abdullahi et al., (2011) carried out integrated geophysical surveys involving 2D electrical resistivity, very low frequency electromagnetic induction method and seismic refraction tomography on Unguwan Dosa municipal solid waste disposal site in Kaduna metropolis, northwestern Nigeria to investigate groundwater contamination. Enikanselu (2008) used electrical resistivity method to investigate the effects of dumpsite on the aquifer units around Giwa – Okearo area of Ogun State. The result obtained indicated that the water from the wells in the area were contaminated. Adebayo et al., (2015) used geophysical approach to delineate contaminant plumes in Ede town, southwestern, Nigeria. They used the electrical resistivity (vertical electrical sounding) and geochemical methods to map the contamination patches at the subsurface and investigate the contamination level of the various hand dug wells in Ede town southwestern Nigeria. Olagunju et al., (2017) used geochemical and geophysical approach to investigate the impact of open dumpsite on the environment. The result showed that the hand dug wells and the river close to the waste dumpsite had been contaminated. In this study, vertical electrical resistivity sounding and electrical resistivity tomography were used to investigate the effects of leachate on groundwater in Gashua, Nigeria. These methods are very suitable for the investigation because, both organic and inorganic chemicals can cause large variations in electrical resistivity of the subsurface.

## **GEOLOGY OF THE STUDY AREA**

Gashua is located within the Chad basin. The Chad basin extends to five countries in Africa, namely, Chad, Nigeria, Cameroon, Central Africa Republic, and Niger. The Basin lies between latitudes  $11^{\circ}$  N and  $14^{\circ}$  N and longitude  $9^{\circ}$  E and  $14^{\circ}$  E, covering Borno State, parts of Yobe and Jigawa States in Nigeria. About ten percent of the Chad Basin lies in the North-eastern part of Nigeria (figure 1). The Chad basin resulted from plate divergence along the

West Africa continental margin (Yikarebogha et al., 2013). The various process which led to the plate divergence started with regional thermal doming, volcanism, rifting, formation of oceanic crust, marine incursion and subsequent widening and deepening of young oceans (Yikarebogha et al., 2013). Sedimentation in the Chad basin started in Albian times, the basal sedimentary sequence is the Bima sandstone, which was deposited unconformably over the Precambrian crystalline basement rock (Yikarebogha et al., 2013). Deposition of the Bima sandstone continued up to the Cenomania. The Turonian was characterized by extensive transgression during which the Gongila Formation was deposited as a transitional sea deposit (Avbovbo et al., 1986). The Fika shale was deposited during the transgression which began in the Turonian and continued up to the senonian period (Matheis, 1976). Towards the end of the Cretaceous, during the Maastrichtian time, an estuarine deltaic environment prevailed in the basin and the Gombe sandstone, shale and limestone were deposited (Yikarebogha et al., 2013). The Keri-Keri Formation was deposited unconformably on the eroded surface of the Gombe sandstone in the Pleistocene (Matheis, 1976). An unconformable Pleistocene deposit of the Chad formation was deposited on the Keri-Keri Formation (Matheis, 1976). The keri-keri formation is eocene in age (ola-Buraimo and Boboye, 2011).

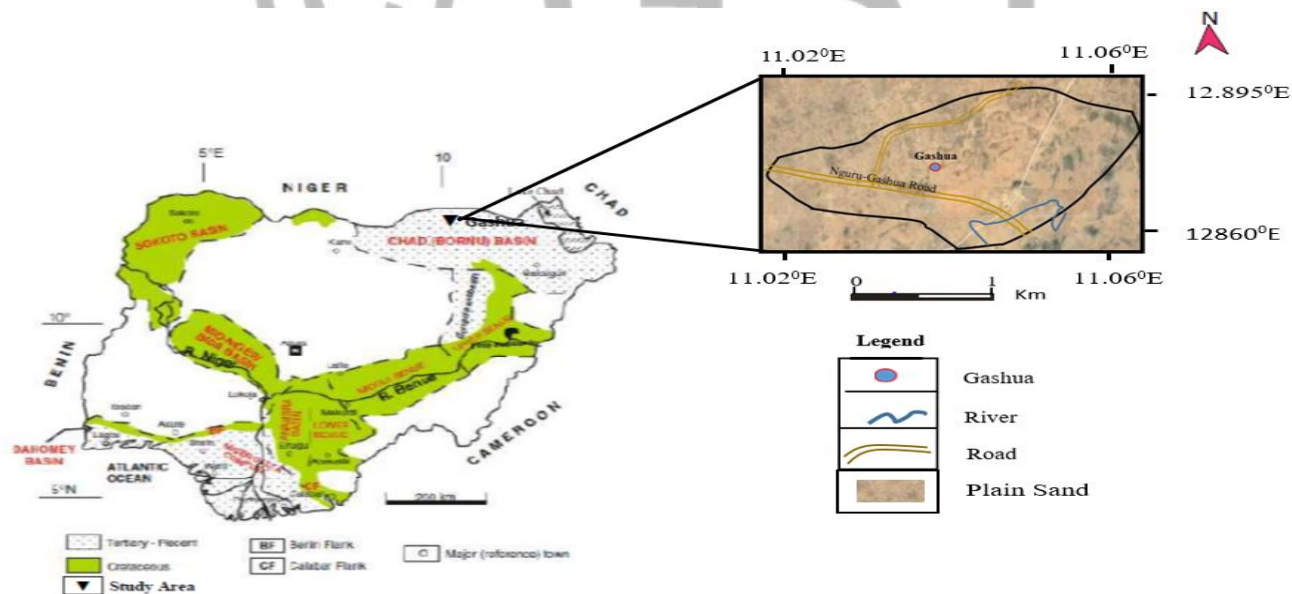


Fig. 1 Geological map of Nigeria (modified after Adebajji, 2012) showing sedimentary basins and the study area.

## MATERIALS AND METHODS

The following instruments were used for the data acquisition ABEM; SAS1000 digital Terrameter, personal computer, Global Positioning System (GPS), Hammers, Measuring tape, UPS Battery and Charger, pegs, ABEM SAS external Battery Adapter (EBA), Electrodes, Reels of Cables and Jumpers.

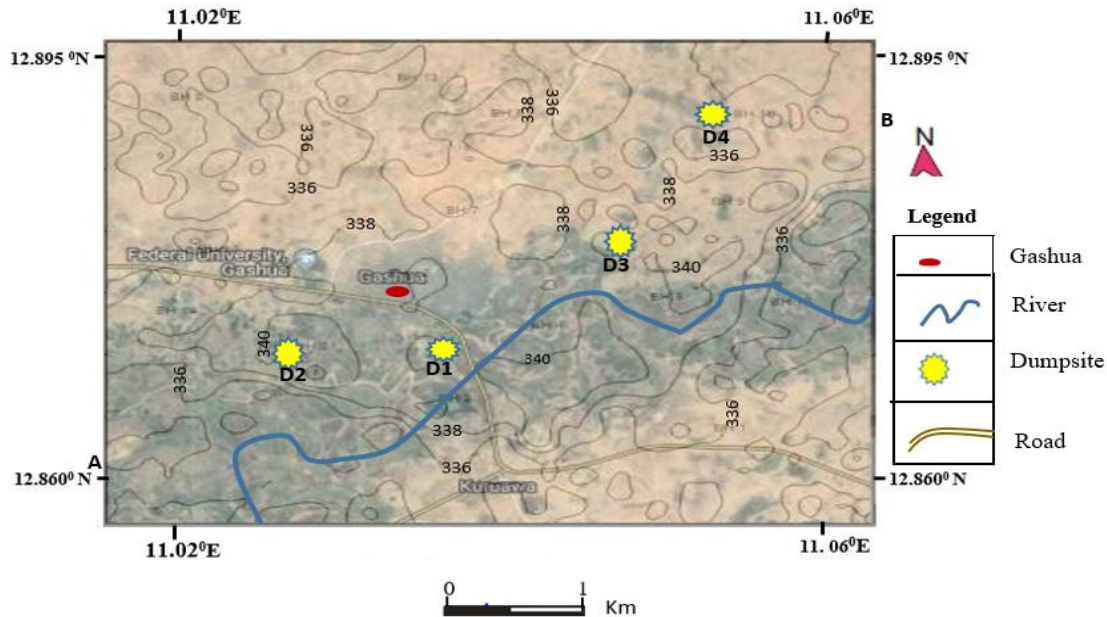


Fig. 2 Sketched Map of Gashua showing selected dumpsites (modified from google maps, 2018).

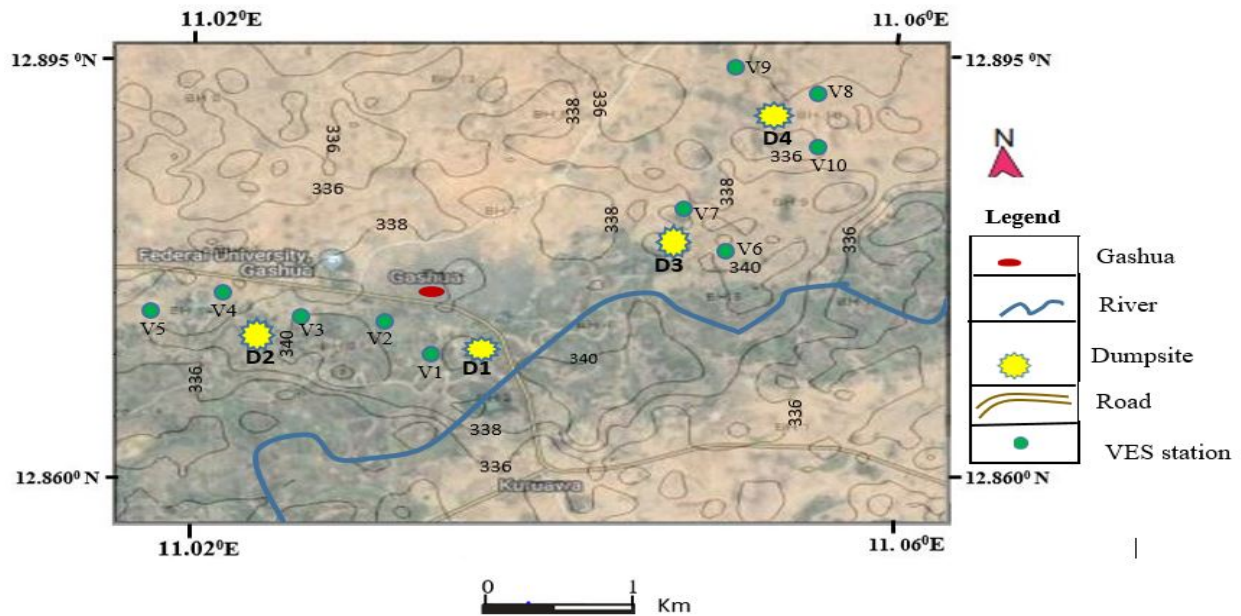


Fig. 3 Sketched of Map of Gashua showing the VES stations.

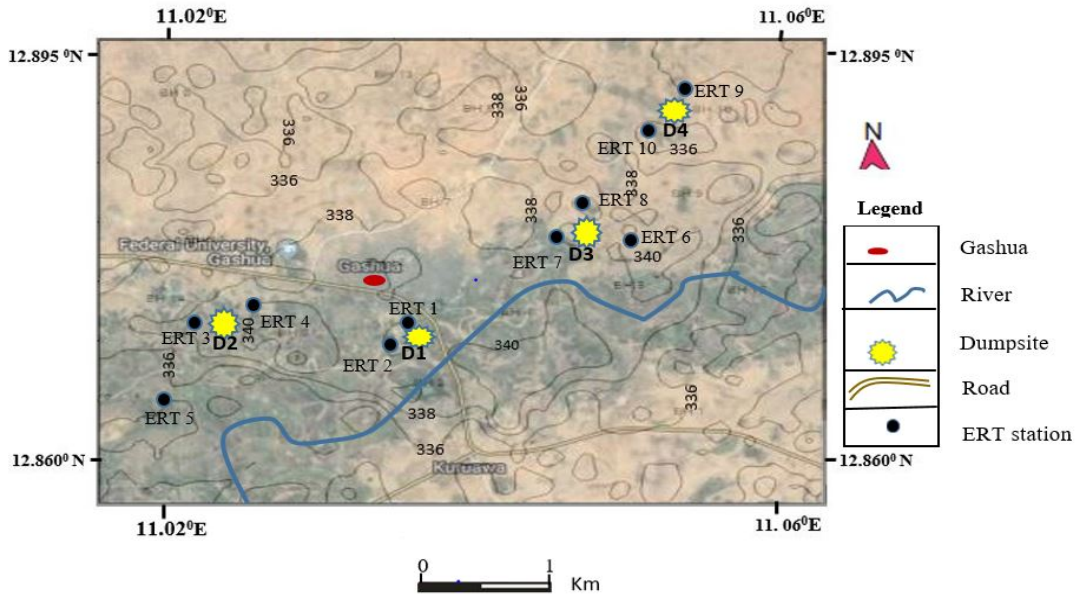


Fig.4 Sketched Map of Gashua showing the ERT stations.

## FIELD PROCEDURE

A total of ten (10) electrical resistivity imaging traverses were measured using 42 electrodes, sets of cable jumpers, hammers and four (4) sets of electrical cables each of 50m length. Wenner Alpha electrode configuration was used to carry out the study with the aid of ABEM SAS1000 Terrameter. During the measurement of the apparent resistivity, the electrical cables were laid along the designed profile and they were then linked to the ground using the electrodes through the sets of cable jumpers. The contact between the electrode cables, electrode take-outs and cable jumpers were checked for proper connections. The electrode test was performed to ensure that current was flowing through all the electrodes. Measurements were made automatically by the Terrameter system and stored with the help of special electrode selection called protocols. This protocol makes series of electrode combinations between the current and the potential electrodes. Files were saved in the Terrameter in binary formats with the file extension\*.s4k. Resistivity measurements for the 2D resistivity profiles were acquired as shown in figure 5.

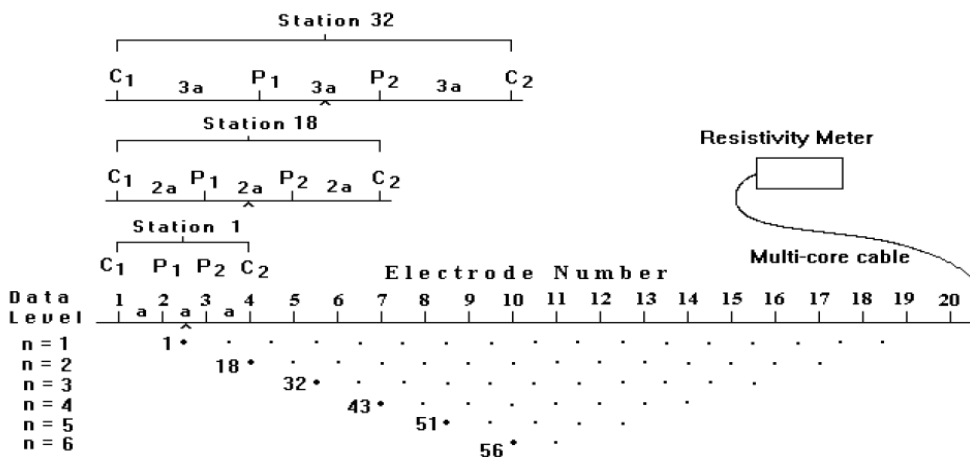


Fig. 5 Sequence of measurements to build up a Pseudo-section (Loke, 1999).

At each measurement, the resistivity meter displayed resistance value and the associated room mean square (RMS) error of the reading. The electrical resistivity tomography (ERT) provide 2D information about the subsurface materials and depth. Ten (10) vertical electrical resistivity sounding was also carried out in the study area using Schlumberger array with the aim of delineating the depth to the groundwater, aquifer thickness and other physical parameters.

### Schlumberger Configuration

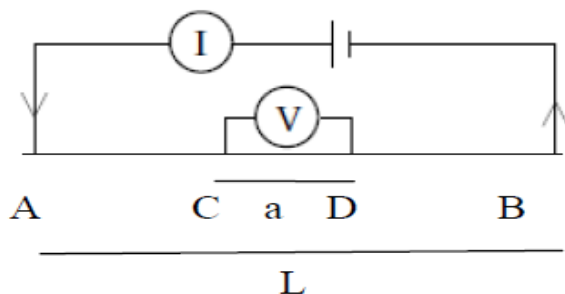


Fig.6 Schlumberger Configuration(Telford, 1990).

The current and potential pair of electrodes often has a common mid-point, but the distances between adjacent electrodes differ. Let the separations of the current and potential electrode be  $L$  and  $a$ , respectively.

$$\text{Then } r_{AC} = r_{DB} = \left(\frac{L-a}{2}\right) \text{ and } r_{AD} = r_{CB} = \left(\frac{L+a}{2}\right).$$

Substituting in these values into the general formula, we have,

$$\begin{aligned} \rho &= 2\pi \frac{V}{I} \left[ \left( \frac{2}{L-a} - \frac{2}{L+a} \right) - \left( \frac{2}{L+a} - \frac{2}{L-a} \right) \right]^{-1} \\ &= \frac{\pi V}{4I} \left( \frac{L^2 - a^2}{a} \right) \quad (1) \end{aligned}$$

The Terrameter measures the resistance, voltage and current which are indicated by  $R$ ,  $V$ ,  $I$  respectively. The apparent resistivity value was obtained by multiplying the resistance by the geometric factor ( $K$ ), that is, ( $R \times K$ ), where  $K$  is calculated by using,

$$K = \frac{\left[ \left( \frac{AB}{2} \right)^2 - \left( \frac{MN}{2} \right)^2 \right] \times 3.142}{\left( \frac{MN}{2} \right) \times 2} \quad (2)$$

Where  $AB$  is the current electrode spacing and  $MN$  is the potential electrode spacing.

During sounding, apparent resistivity of the subsurface material was measured as a function of depth. The progressive increase in the distance between the current electrodes causes the current lines to penetrate to greater depths.

## DATA INTERPRETATION AND PRESENTATION

The recorded data inside the ABEM Terrameter was downloaded in to a personal computer (Laptop) by using a utility software via a communication cable. The downloaded data was then converted from \**.s4k* format into RES2DINV format (\**.DAT* format) which is compatible with the inversion software. The value of the apparent resistivity, electrode spacing and the x-locations were entered in a text file for processing using RES2DINV inversion software (Loke, 1999). The software uses the least square inversion by Quasi-Newton method to achieve the apparent resistivity Pseudo-section (Loke and Barker, 1996). Bad data points were effectively identified as they showed up as stand out points in light of the fact that the apparent resistivity

values were displayed in the form of profiles for every data level. Exterminate bad datum points feature in the RES2DINV software was used to remove negative resistivity values from the data set before the data were inverted. The geoelectrical resistivity inversion software was used to carry out the inversion to produce 2D resistivity model section. The Pseudo-section image of apparent resistivity shows the measured field values. In each image, the horizontal (x) axis represents distance (m) along the surface and also spacing between electrodes while the vertical (Y) axis represents depth (m). Colour legends at the bottom of the image indicate subsurface resistivity values. The acquired vertical electrical sounding (VES) data was presented in the form of tables and were processed using WINRESIST version 1.0. The results from the graph drawn by the processing software shows the thickness, depth and resistivity values of the various soil layers. In the graph, the apparent resistivity values were plotted against the current electrode spacing ( $\frac{AB}{2}$ ) (m) and an iteration process was carried out until a good fit was obtained.

## **RESULTS AND DISCUSSION**

Leachate from the solid waste dumpsite was identified as a great threat to groundwater quality in the study area, they gradually percolate into the subsurface through the vadose zone and migrate into the aquifers where they contaminate the groundwater. The presence of the contaminants in the groundwater was identified by a decrease in the formation resistivity values. The low resistive zones (deep blue) having resistivity ranging from 4.01Ωm to 27.5Ωm were interpreted as leachate contaminants containing toxic substances.

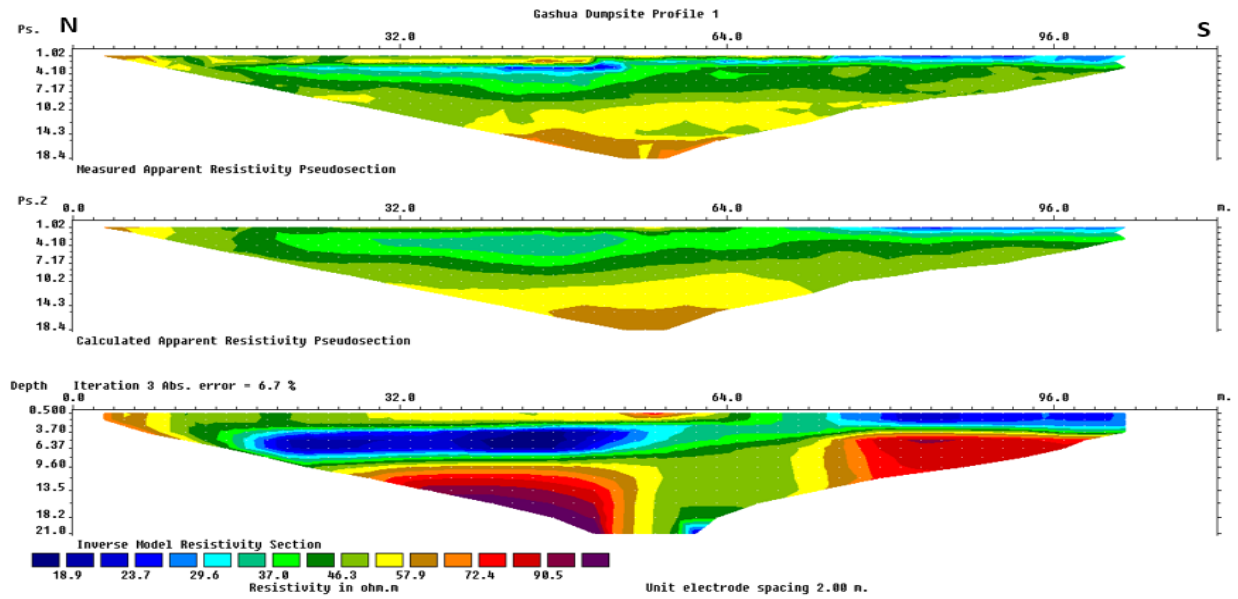


Fig.7 Inverted resistivity model for traverse 1 in the North-South direction of the study area.

Figure.7 shows traverse 1 with a length of 102m in in the North-South direction of the study area. The southern part of traverse 1 is located within the dumpsite and it is characterized by relatively low resistivity values ranging from 18.90Ωm to 29Ωm which manifest as a bowl shape structure within the topsoil. The contaminants migrated from the surface in the southern part to the northern part of the traverse. It manifested at depths ranging from 0.5m to 4.0m in the southern part of the traverse, and from 4.0m to 9.5m in the northern part of the traverse. It was observed to have seeped from the surface points to the depths exceeding 21m within the middle of the traverse.

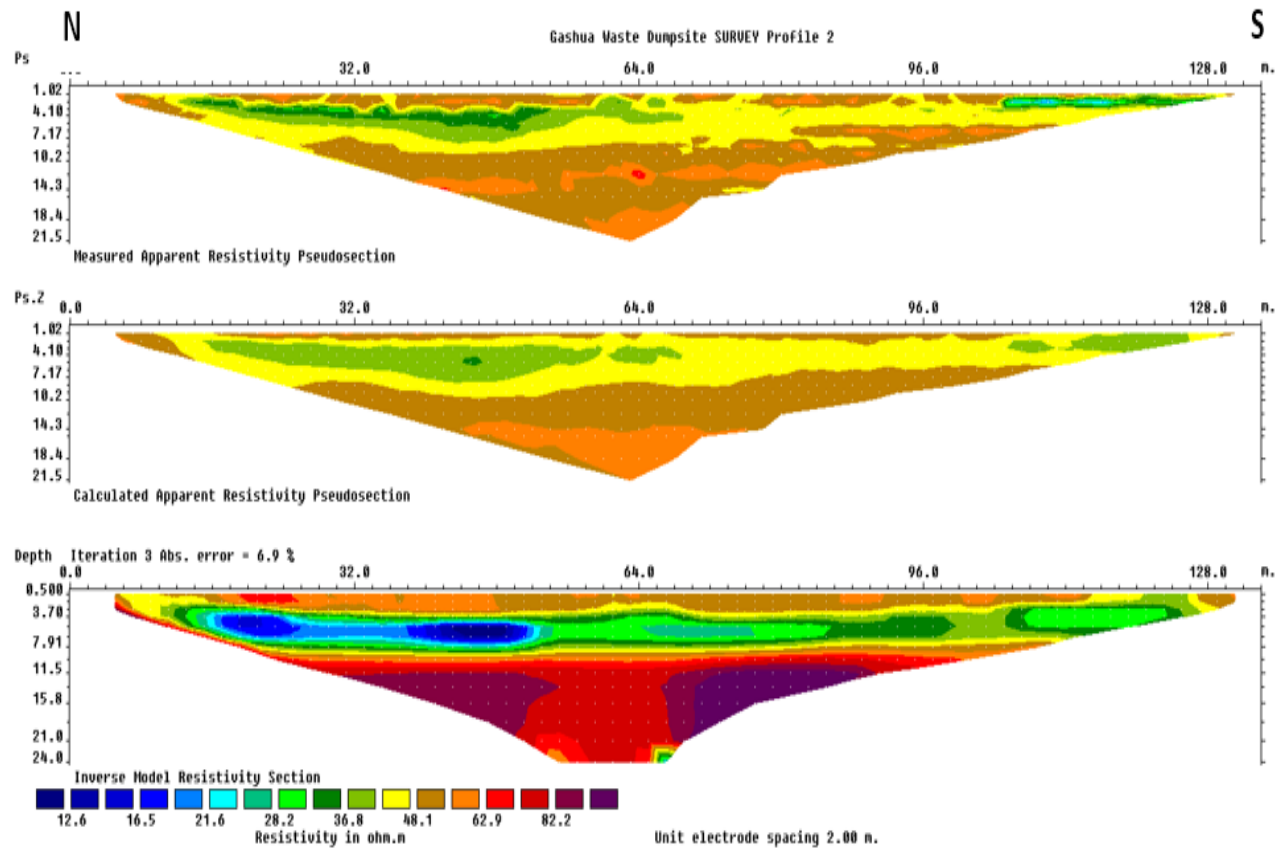


Fig. 9 Inverted resistivity model for traverse 2 in the North-South direction of the study area.

Figure 9 shows traverse 2 with a length of 128m in the North-South direction in the study area. Traverse 2 is located west of dumpsite 1, low resistivity zone was identified in the northern part of profile 2. The resistivity values ranged from 12.6Ωm to 20Ωm with a depth ranging from 3m to 9m and extend from 14m to 54m along the north-south direction.

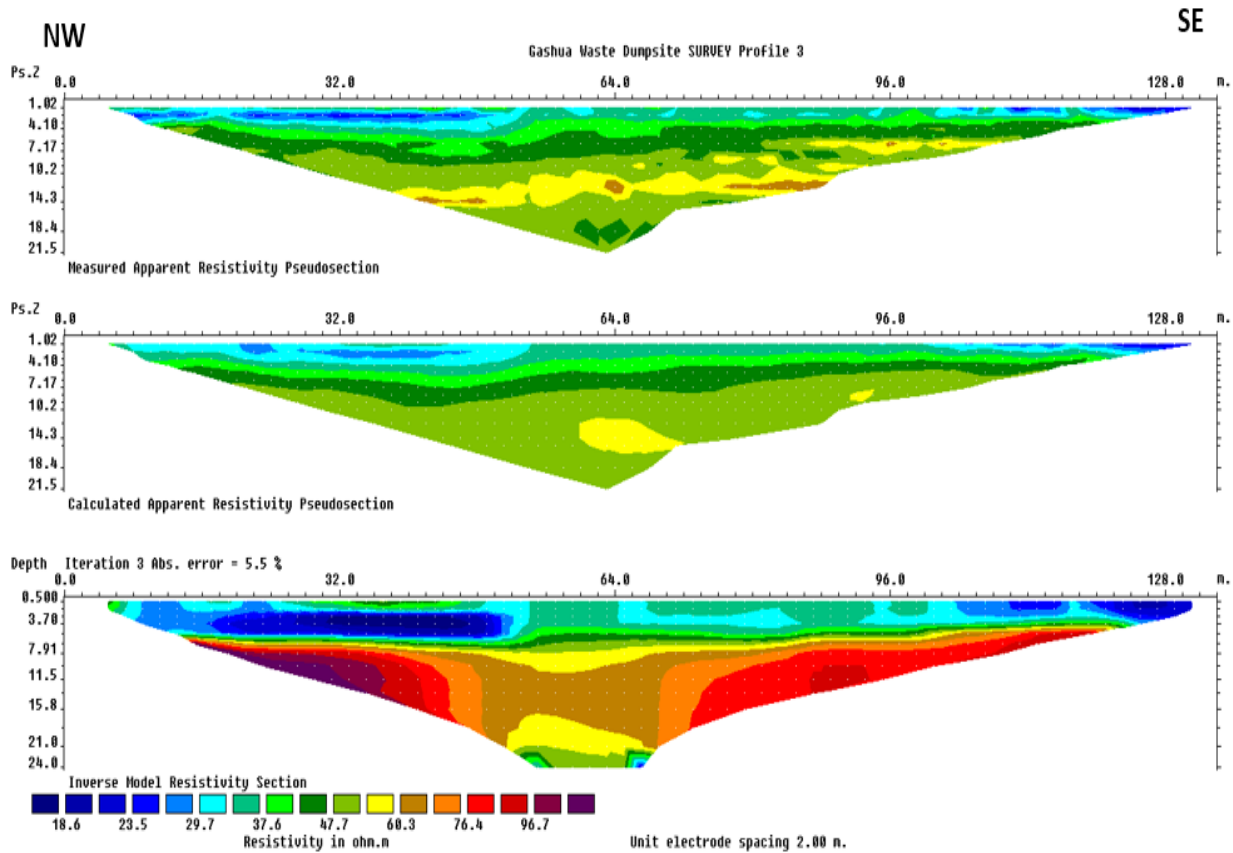


Fig. 10 Inverted resistivity model for traverse 3 in the Northwest-Southeast direction of the study area.

Figure 10 shows model section for traverse 3 comprising of low resistivity anomalies with resistivity values ranging from  $18.6\Omega\text{m}$  to  $24\Omega\text{m}$ , an indication of leachate at horizontal distance of 8 – 42m and 104 – 130m. The resistivity values throughout the traverse section were less than  $100\Omega\text{m}$ . The traverse has a length of 130m and trend northwest – southeast direction in the study area. The contaminant plume had seeped from the surface to a point beyond 24m deep. It might have impacted the groundwater in the study area.

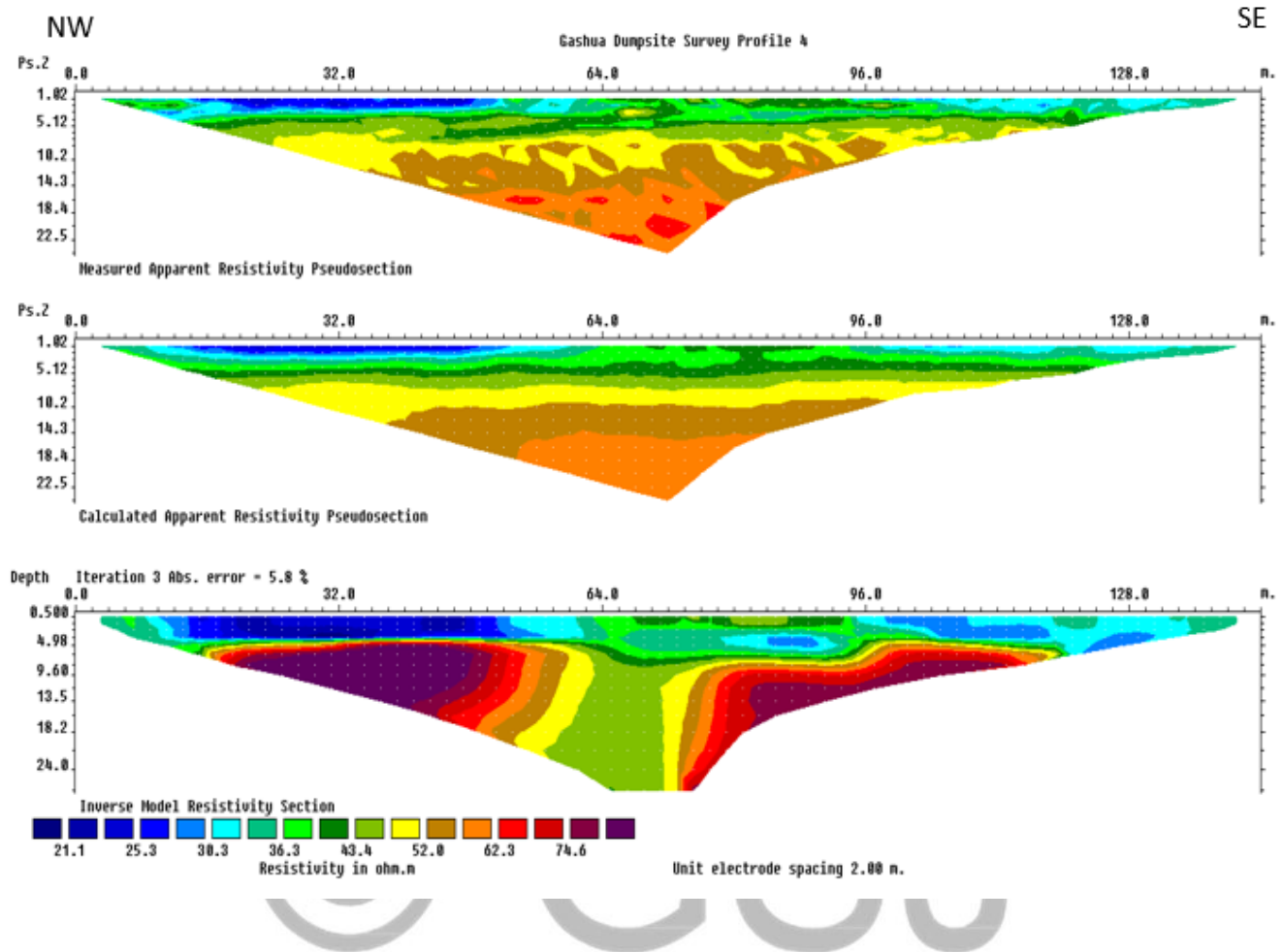


Fig.11 Inverted resistivity model for traverse 4 in the Northwest-Southeast direction of the study area.

Figure 11 shows traverse 4 with a length of 140m in a Northeast – Southwest direction to the study area. It was observed from the traverse that this part of the study area is made up of continuous horizontal spread of leachate plume from the ground surface to a depth of 10m deep. The leachate might likely seep deeper into the subsurface with time. The leachate migration in this area originates from the northwestern end of the traverse and extends to the southeastern part of the traverse. The leachate is characterized with resistivity values ranging from 20 - 25Ωm.

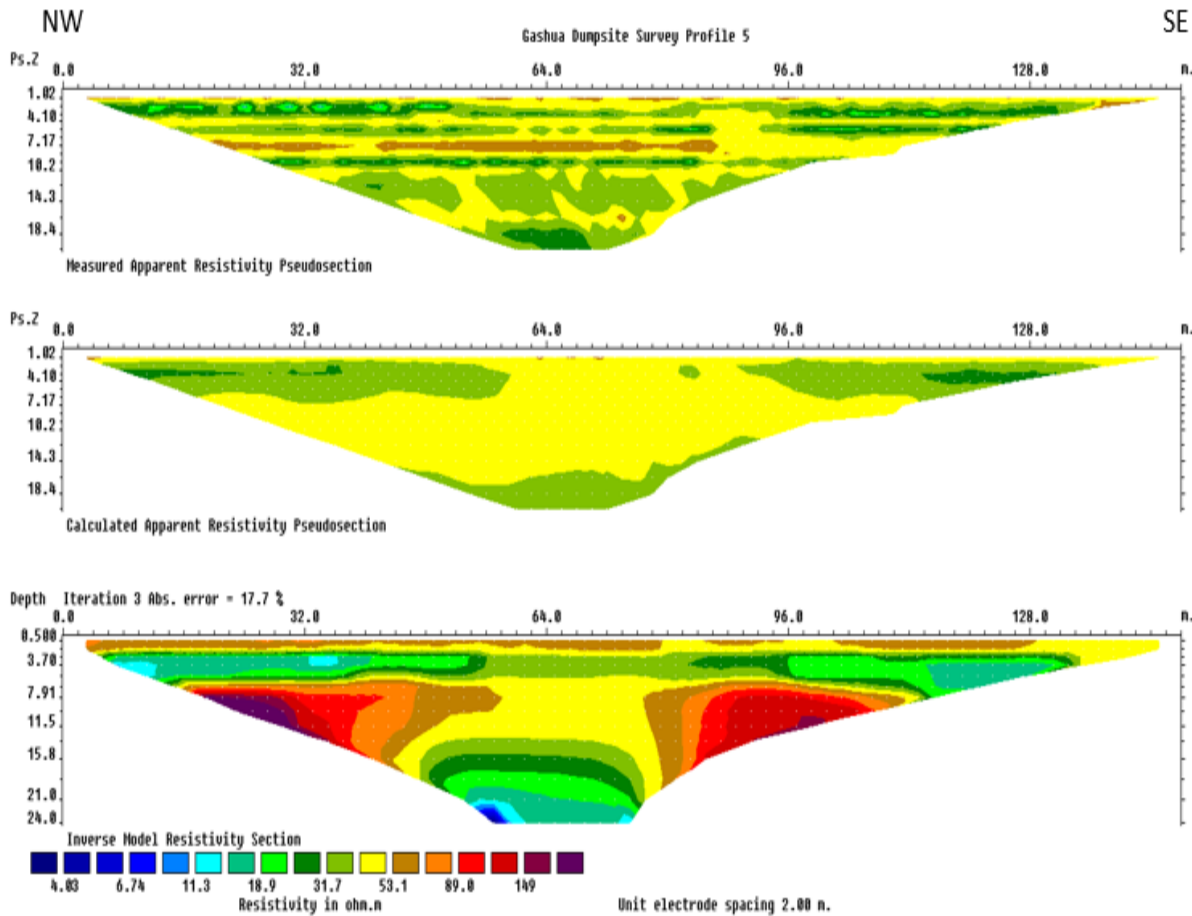


Fig. 12 Inverted resistivity model for traverse 5 in the Northwest-Southeast direction of the study area.

The inverse model section of traverse 5 is the control traverse which is shown in figure 12. The topsoil is characterized with moderately high resistivity values along the horizontal spread which is an indication of non-invasion of the area by contaminant plume. The sandy clay and sand formations below the topsoil were free of contamination. But at a depth beyond 22m in the subsurface within the middle of the traverse there is an isolated low resistivity anomaly whose value ranged from 4 - 11 $\Omega$ m. The presence of the anomaly indicates that the contaminant plume might have migrated from a distance dumpsite to the domain of traverse 5. The contaminant plume is suspected to have contaminated the groundwater in the area because of its deep location within the area.



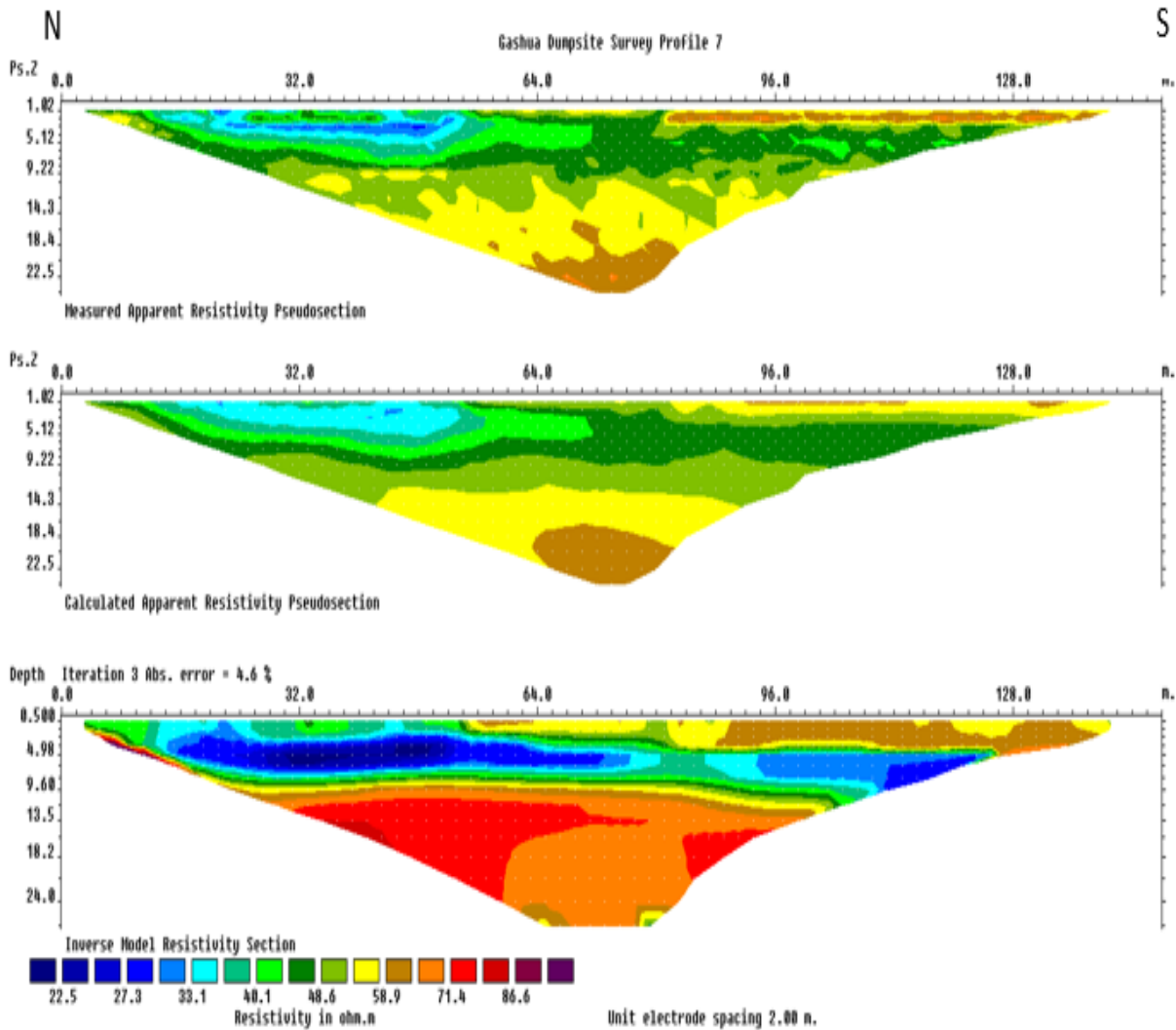


Fig.14 Inverted resistivity model for traverse 7 in the North -South direction of the study area.

The inverse model section of traverse 7 shows low resistivity values between 22 and 27Ωm in figure 14 above. The low resistive anomaly indicated in a deep blue colour is an evidence of leachate contaminant plume formation with nearly uniform horizontal and depth extent. The contaminant plume originates from the surface and migrate from the northern side of the traverse towards the southern part. The leachate plume migrated from the dump site and infiltrated the area to a depth greater than 10m below the dump. Below the leachate invaded area is a sandy clay formation which helped to impede the leachate migration. Under the sandy clay formation lies the sand formation with resistivity values ranging from 50 - 85Ωm. This formation is highly porous and could easily be invaded by the contaminant plume.

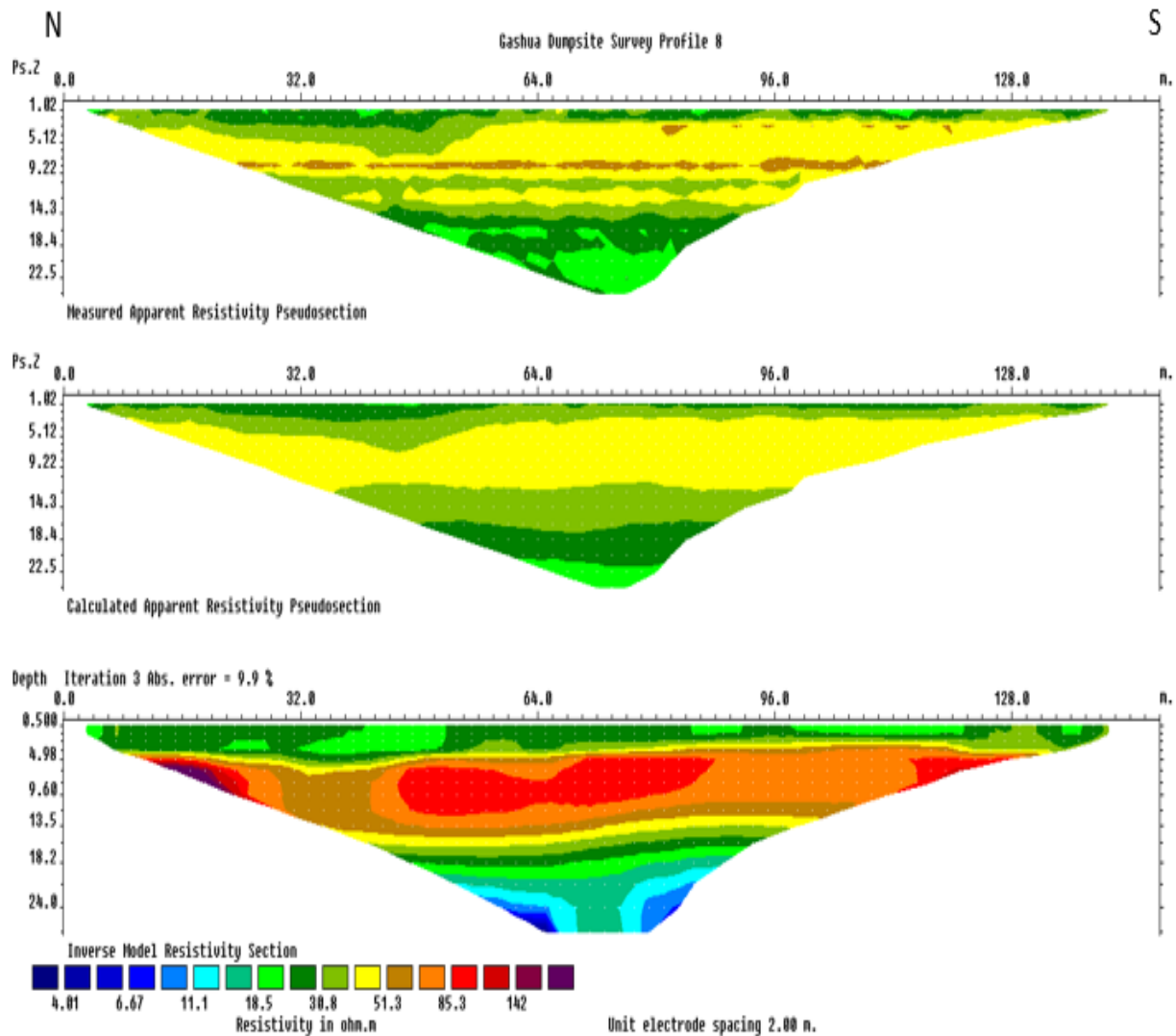


Fig. 15 Inverted resistivity model for traverse 8 in the North -South direction of the study area.

The inverted resistivity model for traverse 8 showed two resistivity anomalies in figure 15 above. The resistivity values of the anomalies ranged from  $4\Omega\text{m}$  to  $11\Omega\text{m}$  and the anomalies which are interpreted as leachate contaminant plumes manifested from a depth of 22m and went deeper into the subsurface. The contaminant plume migration to the deeper part of the subsurface is enhanced by the porous and permeable nature of the dominant sandy formations of the aquifer materials. This contaminant plume that occur deep in the subsurface in the study area might have polluted the groundwater.

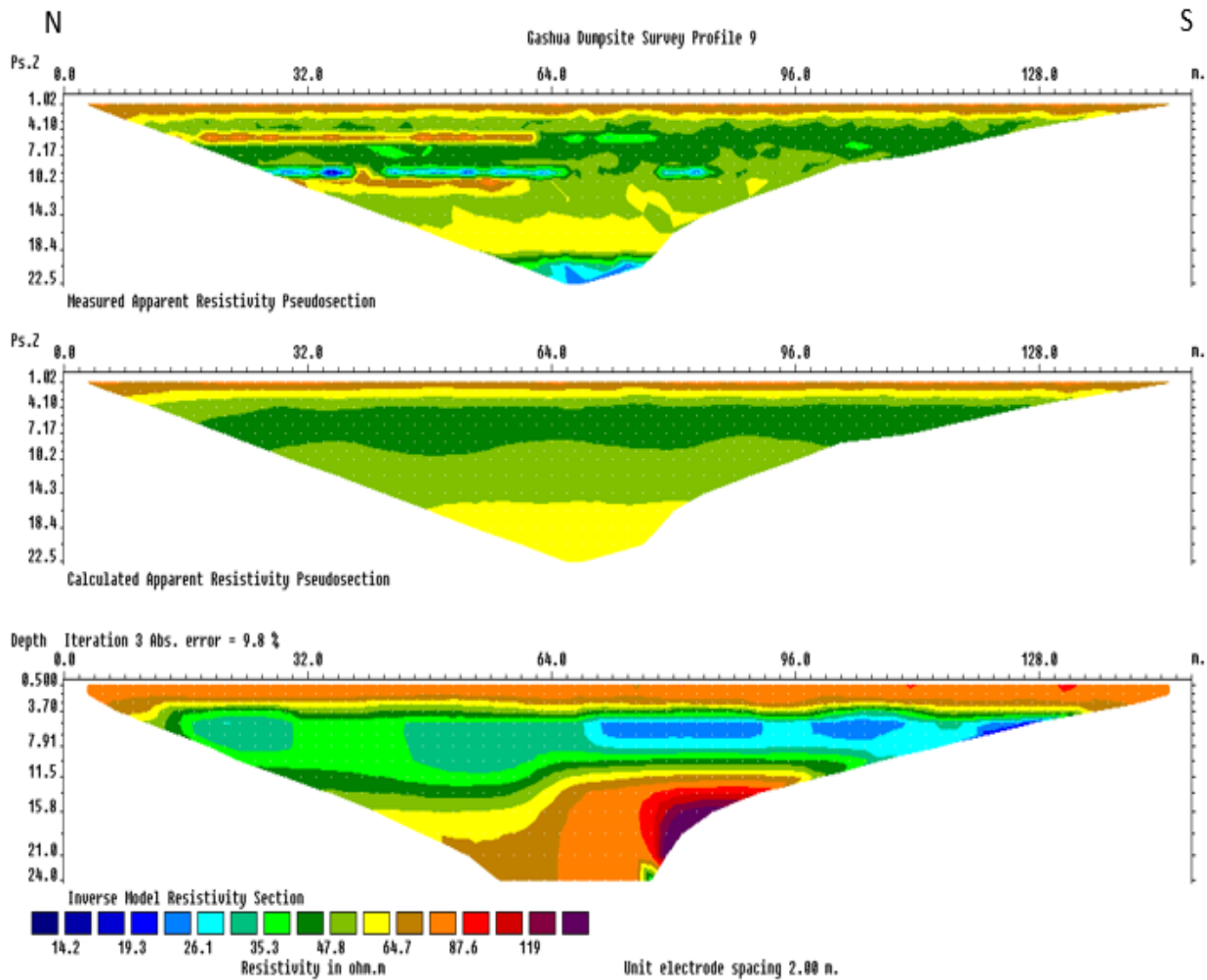


Fig. 16 Inverted resistivity model for traverse 9 in the North-South direction of the study area.

Figure 16 shows the model section for traverse 9 which has low resistivity anomalies with resistivity values ranging from  $14\Omega\text{m}$  to  $20\Omega\text{m}$ , the anomaly is an indication of leachate contaminant plume which occur at horizontal distance of 70 to 128m towards the southern direction in the study area. The contaminant plume manifested at a depth of 5m below the surface and extends to a depth of 10m deep. Following this plume is a sandy clay at depth of 10 to 13m with resistivity values ranging from 30 to  $50\Omega\text{m}$  indicated in green colour in figure 16. Beyond this zone is the sandy formation with resistivity values ranging from 60 to  $120\Omega\text{m}$  indicated in yellow, brown and purple colour in figure 16 above. The sandy formation is prone to groundwater contamination as the dumpsite ages.

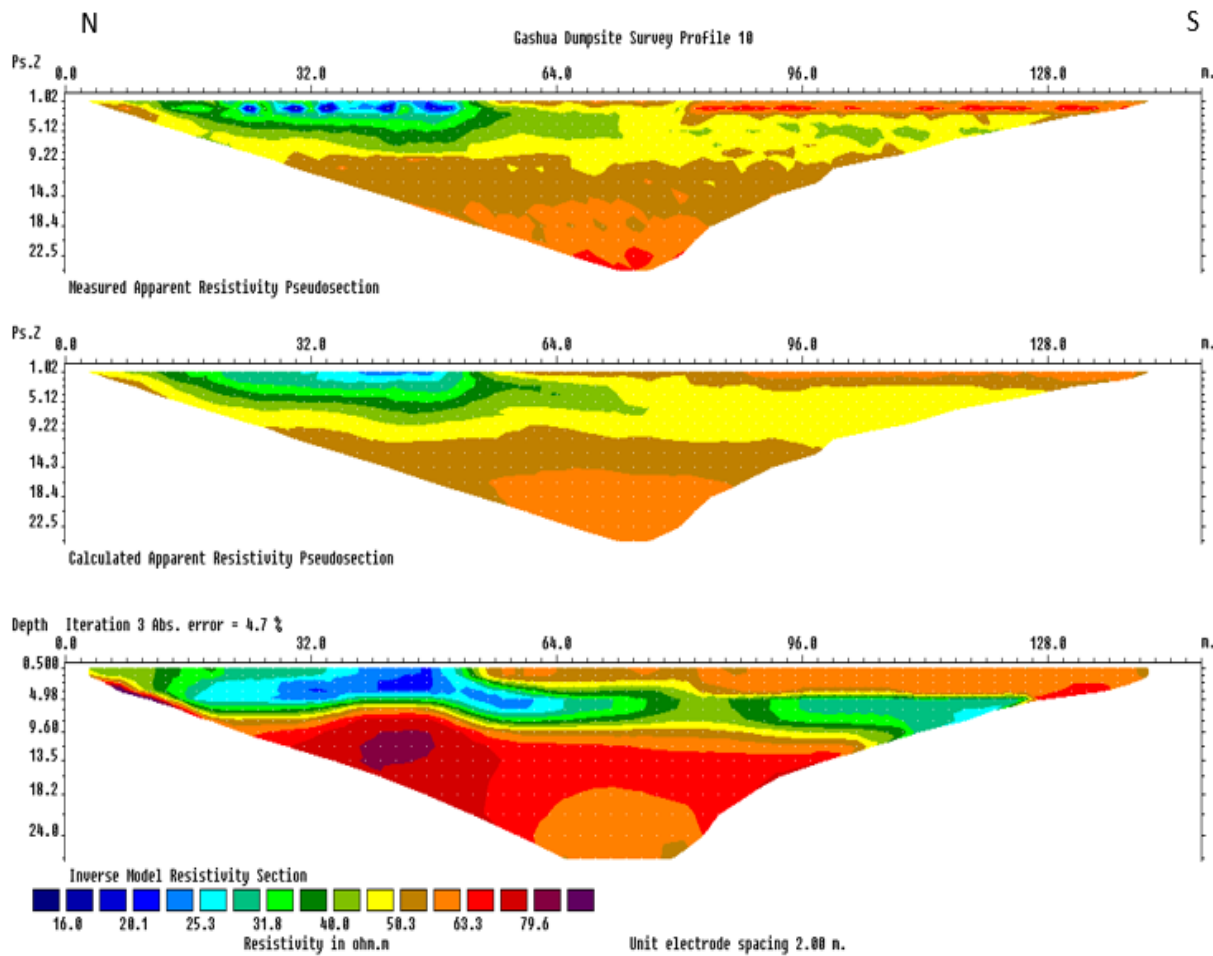


Fig.17 Inverted resistivity model for traverse 10 in the North-South direction of the study area.

The inverse section of profile 10 is shown in figure 17, the 2D section shows low resistivity anomaly towards the northern part of the traverse at position 34 – 52m and spread deep into the subsurface. The anomaly is characterized by resistivity values ranging from 16 to 22Ωm as shown in figure 17 in deep blue colour. The anomaly is a leachate contaminant plume which migrate from the surface to a depth of about 6.5m below the surface. It has not penetrated deeper into the subsurface, but as the dump ages with stead percolation of leachate into the subsurface, the contaminant plume will reach the groundwater zone and spread across the area.

## **GEOELECTRIC SECTIONS.**

Figures 18 and 19 show the Geoelectric sections for VES 1, 2, 3, 8, 9 and VES 4, 5, 6, 7 and 10 around the four solid waste dumpsites in the study area. To greater extent, the results show good correlation in terms of number of layers when compared with an existing borehole log (figure 20). The VES results are presented as the resist graph/VES curves (Appendix A). Several iterations were carried out to ensure low root mean square (RMS) and accuracy of the results. The results of the VES helped in characterizing the subsurface geology around the dumpsite (figures 18 and 19). The geologic layers delineated were characterized into five layers (table 1). These are; the topsoil, clay, sand, sandy-clay and sand. The topsoil has resistivity ranging from 42.7 to 199.7 $\Omega$ m and 0.6 to 1.9m thickness, the second layer is a clay formation which has resistivity ranging from 16.5 to 37.9 $\Omega$ m and thickness ranging from 4.1 to 10.7m. The second layer is characterized with low resistivity values suggesting the presence of clay mixed with non-degradable contaminant. This observation is consonance with the results of the ERT survey discussed earlier. The ERT results showed that the contaminant plume is most prominent within shallow depth in the study area. The clay content in the second layer is minimal and the thickness of the layer in all the VES points is generally small, thus providing little or no protection to the aquifer beneath them. The sand formation whose resistivity ranges from 101.2 to 288.2 $\Omega$ m is the third layer with thickness ranging from 38.9 to 99.7m. It is the first aquifer in the study area where all the hand dug wells and shallow boreholes were drilled. It is vulnerable to pollution by contaminant plume considering its shallow nature, porosity, permeability and dominance of sand formation in the study area. The third layer is unconfined and it is highly susceptible to pollution from leachates. The fourth layer is made up of sandy-clay which has resistivity values ranging from 100.7 to 214.3 $\Omega$ m with thickness ranging from 28.5 to 94m.

The fifth layer is under confined condition provided by the fourth layer. This layer is the most important groundwater unit in the study area and its resistivity value range from 254 to 350 $\Omega$ m. It is a sandy aquifer with great thickness. Depths of boreholes in the study area were found to range from 60m to 120m while the average depth of hand dug wells in the study area is 20m (Makinde et al., 2010).

Table 1 Vertical Electrical Resistivity Sounding Results.

VES Station	Longitude (°E)	Latitude (°N)	Resistivity ( $\Omega\text{m}$ )					Thickness (m)				Depth (m)			
			$\rho_1$	$\rho_2$	$\rho_3$	$\rho_4$	$\rho_5$	$h_1$	$h_2$	$h_3$	$h_4$	$d_1$	$d_2$	$d_3$	$d_4$
1	11.03716	12.86309	91.1	26.7	213.4	104.8	260.6	0.8	6.7	44.4	58.6	0.8	7.5	51.9	110.5
2	11.03493	12.86468	109.4	19.9	288.2	100.7	314.8	1.4	5.5	38.9	66.7	1.4	6.9	45.8	112.5
3	11.03205	12.86585	111.3	31.7	101.2	214.3	281.4	1.0	5.0	46.5	49.0	1.0	6.0	45.8	101.5
4	11.05085	12.86610	42.7	30.1	101.4	171.4	318.7	1.1	4.3	58.6	28.5	1.1	5.4	64.0	92.5
5	11.04965	12.86769	59.9	15.9	266.9	125.3	291.8	1.6	4.1	73.4	47.5	1.6	5.7	79.1	126.6
6	11.05257	12.87476	169.3	25.1	242.0	118.1	253.8	1.1	7.0	44.1	30.5	1.1	8.1	52.2	82.7
7	11.05047	12.87476	113.3	32.4	194.8	149.7	306.3	1.9	10.3	45.6	29.5	1.9	12.2	57.8	87.0
8	11.02919	12.86705	107.5	16.5	189.7	136.5	350.1	1.4	4.5	99.7	37.6	1.4	5.9	105.6	143.2
9	11.02538	12.86880	189.3	29.9	196.0	184.1	307.4	0.6	7.0	50.5	94.0	0.6	7.6	58.1	152.1
10	11.05348	12.87127	199.7	37.9	274.1	132.8	326.8	0.8	10.7	46.9	69.4	0.8	11.5	58.4	127.8

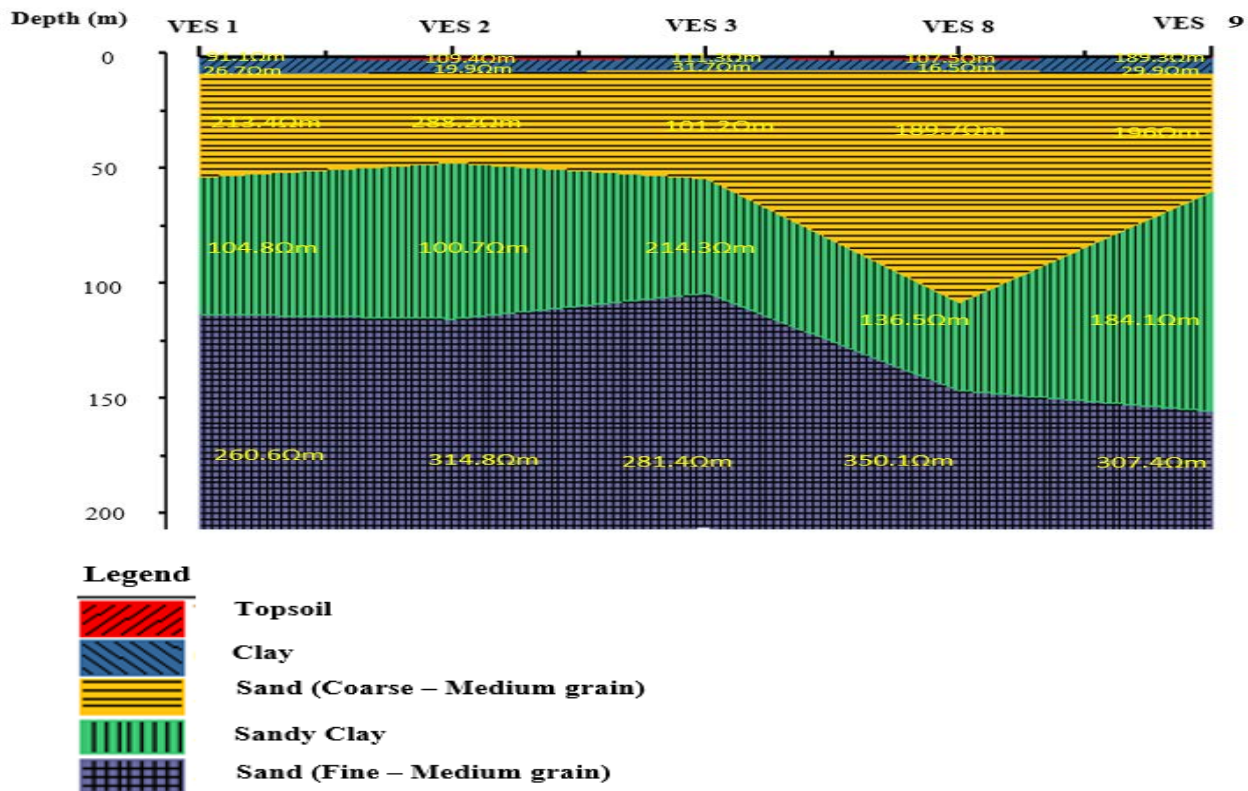


Fig. 18 Geo-electric section of VES 1, 2, 3, 8 and 9 in the Northeast-Southwest direction towards dumpsites 1 and 2.

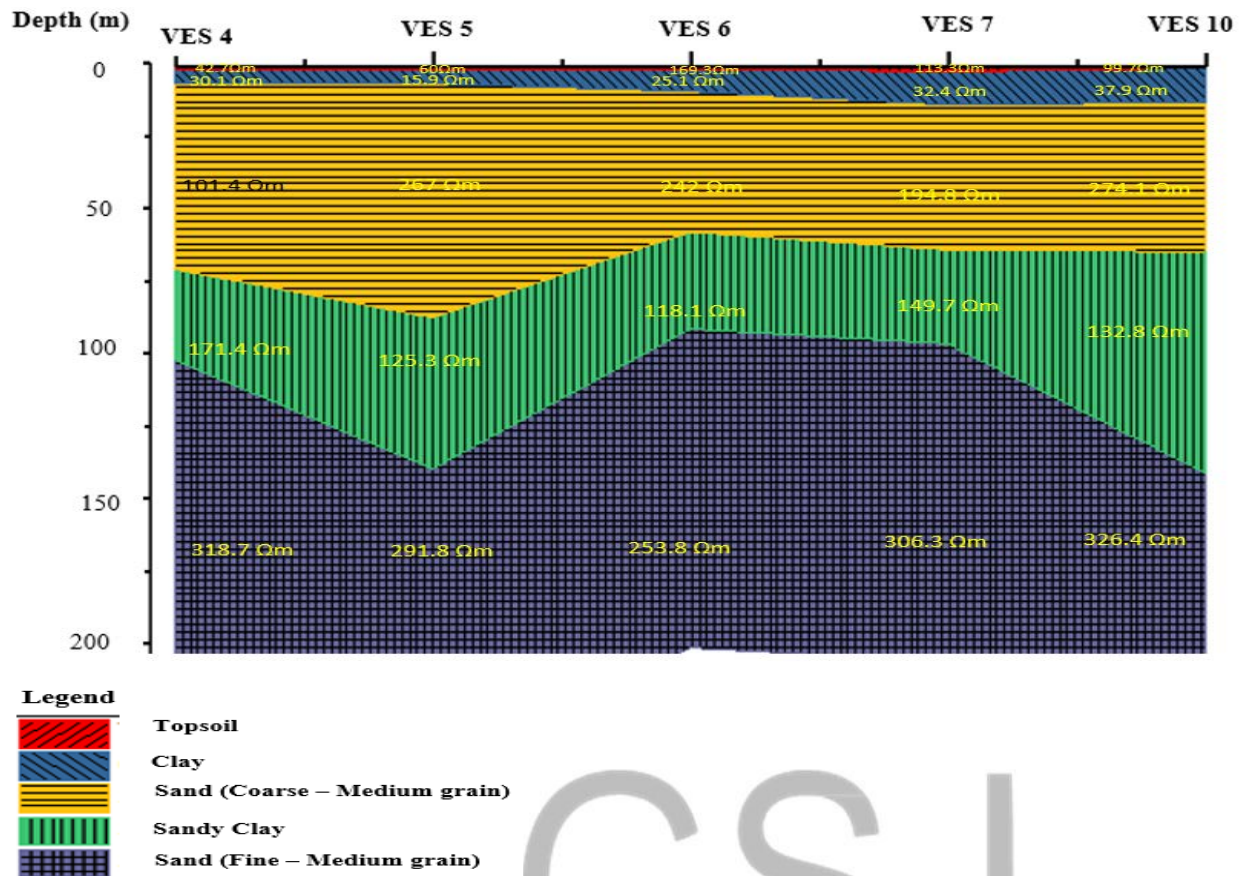


Fig.19 Geo-electric section of VES 4, 5, 6, 7 and 10 in the Northeast-Southwest direction towards dumpsites 3 and 4.



Fig. 20 Typical borehole log of Katuzo in Gashua (Modified from Ministry of Water resources Damaturu).

### Contaminant Flow Direction

The contaminants flow direction was determine by obtaining the elevation profile section of the study area using the topographic map of the area. The elevation profile section shows that the contaminant plume flow from Southwest to the Northeast of the study area.

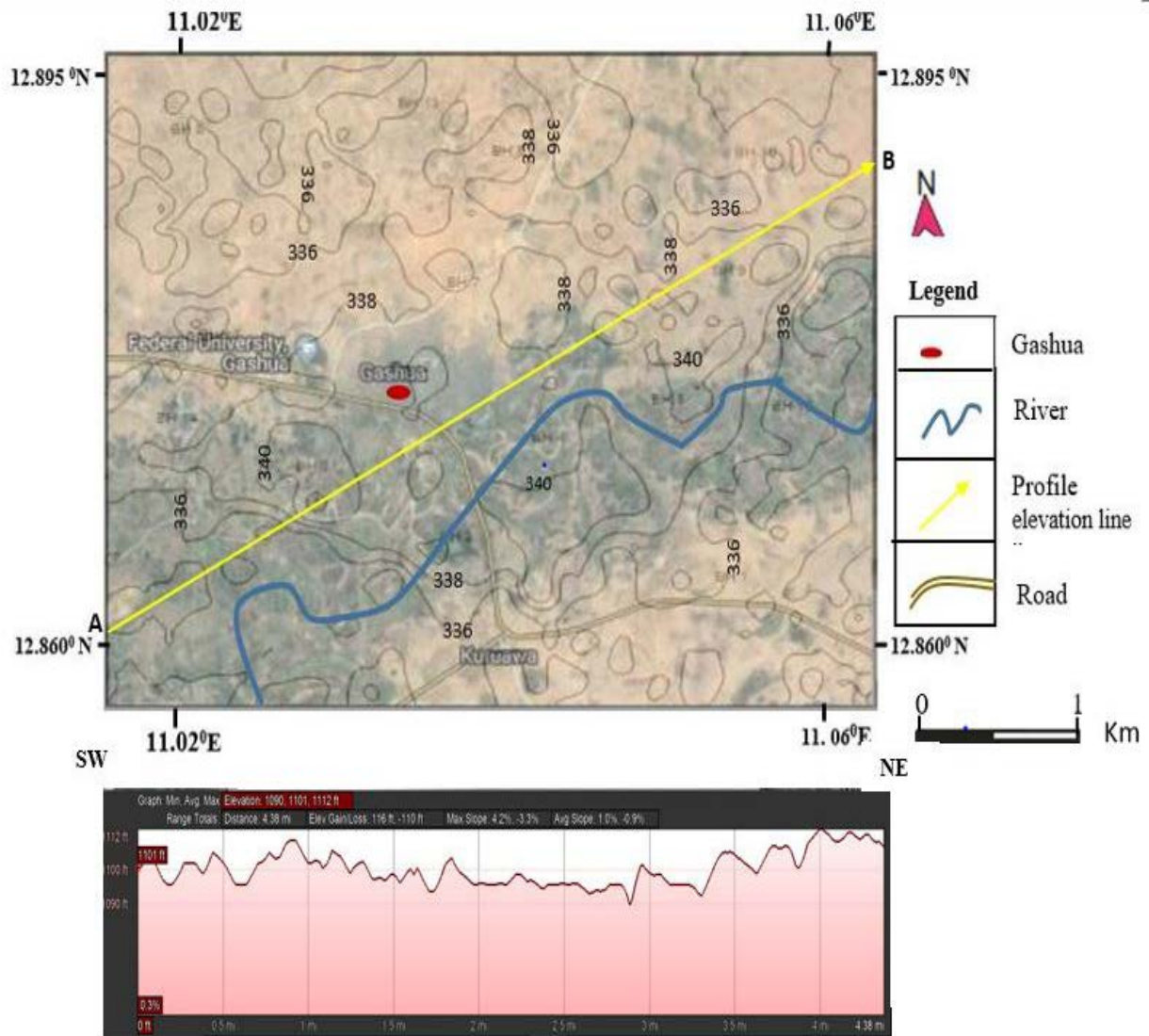


Fig. 21 Elevation contour map showing the direction of contaminant flow.

The contaminant flow in the study area is aided by the dominant sandy formation which constitute the first aquifer in the study area. Results of the electrical resistivity survey showed that the first aquifer is unconfined, therefore the contaminants easily seep into the groundwater.

## CONCLUSION AND RECOMMENDATIONS.

The analysis of all the geophysical results obtained from the study area indicate that leachate from the solid waste dumpsites has infiltrated the sandy aquifers and therefore polluted the groundwater in the area. Water from hand dug wells and boreholes located within the contaminated zones could be responsible for high prevalence of water related diseases in the study area. The average depth of hand dug wells in the study area is 20m. Several of the boreholes were sited within the first aquifer which is unconfined, and this situation makes them vulnerable to pollution by leachate from the dumpsites. The 1D vertical electrical resistivity sounding and the 2D ERT results showed that the aquifers in the study area are contaminated by leachate from solid waste dumpsites. Base on the findings of this study, the following are therefore recommended.

- i. Deeper drilling and constant monitoring of borehole water should be encouraged.
- ii. Government should enforced environmental protection laws that will prohibit indiscriminate disposal of solid waste material from domestic and industries.
- iii. Effective sanitation should be put in place to mitigate the source of contaminant to the ground water.
- iv. Adequate geophysical investigation should be carried out to understand the nature of the aquifer in which boreholes are to be sited for drinking water in the study area. Perfectly confined aquifers are preferable in a sandy environment such as the study area to overcome the problem of leachate percolation into the groundwater.
- v. The consumption of water from hand dug wells and shallow boreholes should be discourage in the study area. Boreholes close to the dumpsites should be closed and new ones should be sited at distances far from the dumpsites to avoid pollution.
- vi. Sensitization workshops and public awareness programmes on dangers of consumption of contaminated water should be carried out.

## REFERENCES

Abdullahi, N.K., Osazuwa, I.B. & Sule, P.O. (2011): Application of Integrated Geophysical techniques in the investigation of groundwater contamination. A case study of municipal solid waste leachate. *Ocean Journal of Applied Science*. 4(1), 7-25.

- Adebanji, K. A. (2012). Biostratigraphy and Depositional Environment of the sediments in Borno Basin, Northeastern Nigeria. *International Journal of Science and Technology*, 5: 2800-2809.
- Adebayo, A.S., Ariyibi, E.A., Awoyemi, M.O. & Onyedim, G.C. (2015). Delineation of contamination plumes at Olubonku dumpsite using geophysical and geochemical approach at Ede town, southwestern Nigeria. *Niger Geosci* 5(1), 43-54.
- Amidu, S.A., & Olayinka, A.I. (2006). Environmental assessment of sewage disposal system using 2D electrical resistivity imaging and geochemical analysis. A case study of Ibadan, southwestern Nigeria. *Environ Eng. Geosci.* 12, 261- 272.
- ATSDR, Agency for Toxic Substances and Disease Registry (2000). *Toxicological profile for chromium*. Atlanta, GA: US department of Health and Human Service, Public Health Service.
- Avbobvo, A. A., Ayoola, E.O., & Osahon, G. A. (1986). Depositional and structural styles in Chad Basin, Northeastern Nigeria. *AAPG Bull*, 70, 1788-1798.
- Bernstone, C., & Dahlin, T. (1999). Assessment of two automated DC Resistivity Data acquisition systems to landfill location surveys. *Journal of Environmental and Engineering Geophysics*. 4(2), 113-121.
- Cristina, P., Cristina, D., Alicia, F., & Pamela, B. (2012). Application of Geophysical methods to waste disposal studies, municipal and industrial waste disposal studies. Dr. Xian-Ying Yu (Ed) ISBN 978-953-51-0501-5.
- Enikanselu, P.A. (2008). Detection and Monitoring of Dumpsite Induced Groundwater Contamination using Electrical Resistivity Method. *Pacific Journal of Science and Technology*, 9(1), 254-262.
- Freeze, R.A., & Cherry, J.A. (1979). *Groundwater*. Prentice –Hall. Englewood Cliffs, pp.29-118. Faure, G. (1986). *Principles of isotope geology*, 2<sup>nd</sup> Ed., John Wiley & Sons, New York,

- Google Maps. (2018). Topographic map of Gashua, Yobe State Nigeria (modified). Retrieved from [https:// www.google.com /maps / d/viewer? mid = ZiZA4Hopius KEJc02G0F04&ie = UTF 8&0e=UTF8 & msa = 0](https://www.google.com/maps/d/viewer?mid=ZiZA4HopiusKEJc02G0F04&ie=UTF8&msa=0).
- Keller, G.V. & Frischescht, F.C. (1999). *Electrical methods in Geophysics prospecting*. New York: Pergamon Press Inc.
- Loke, M.H. (1999). Time-lapse resistivity imaging inversion. Proceedings of the 5<sup>th</sup> Meeting of the Environmental and Engineering Geophysical Society European Section, Em1.
- Loke, M. H. and Barker, R. D.,(1996). Practical techniques for 3D resistivity surveys and data inversion. *Geophysical Prospecting*, 44, 499 - 523.
- Makinde, V., Alagbe S.A, Coker, J.O., & Bello, A.M.A. (2010). Determination of borehole sites for extensive irrigation work in Yobe State, Nigeria. *Journal of American Science*, 6(2), 58-61.
- Matheis, G. (1976). Short review of the Geology of the Chad Basin in Nigeria. In C.A. Kogbe (Ed.) *Geology of Nigeria*. Lagos: Elizabeth publishing company.
- Ola-Buraimo, A.O., & Boboye O. A. (2011). Palynological investigation of the Albian to lower Cenomanian Bima Formation Borno, Nigeria. *World Applied Science Journal*, 12 (17) 1026-1033.
- Oladunjoye, M.A., Olayinka, A.I. & Amidu, S.A. (2011). Geoelectrical Imaging at an Abandoned Waste dump site in Ibadan, Southwestern Nigeria. *Journal of Applied Science*, 11(22), 3755 - 3764.
- Olagunju, E., A., Emmanuel, M., Awoyemi, A., Adebayo, O., Dasho, C., A. (2017). Application of geochemical and geophysical approach to environmental impact assessment: A case study of Emiran active open dumpsite, Ado-Ekiti southwestern Nigeria. *Model Earth Syst. Environ.* DOI 10.1007/S4080801703811.
- Olayinka, A.I., & Olayinwola, M.A. (2001). An integrated use of geoelectric imaging and hydrogeochemical methods in delineating limits of polluted surface and groundwater at landfill site in Ibadan area southwestern Nigeria. *Journal of Mining and Geology*, 37(1) ,53-68.

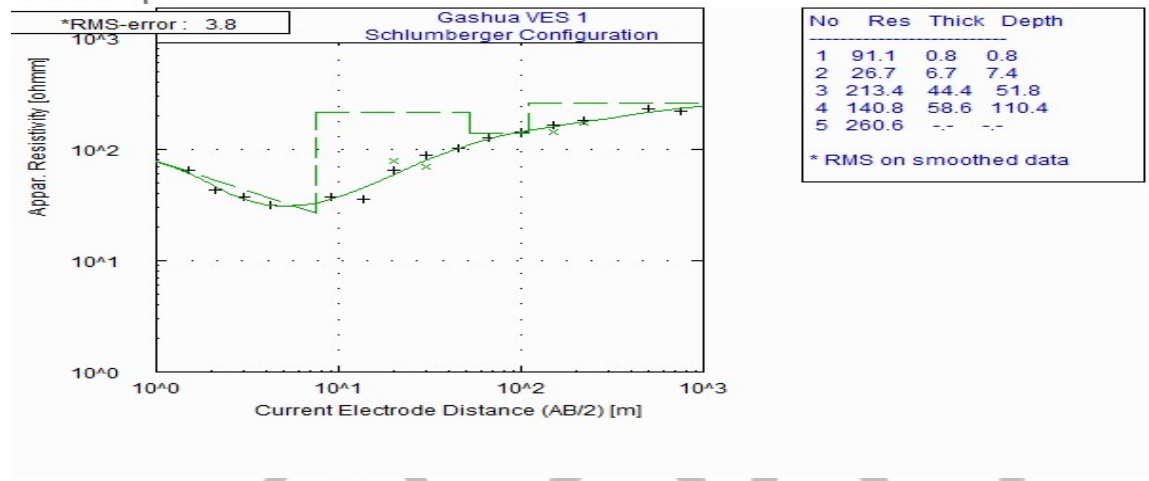
Telford, W.M., Geldart, L. P. & Sheriff, R. E. (1990). *Applied Geophysics* (2nd edition),  
 Cambridge: Cambridge Univ. press

Yikarebogha, Y., Oloto, I.N., Soronnadi- Ononiwu, G. C., & Omoboriowo, A. O. (2013).

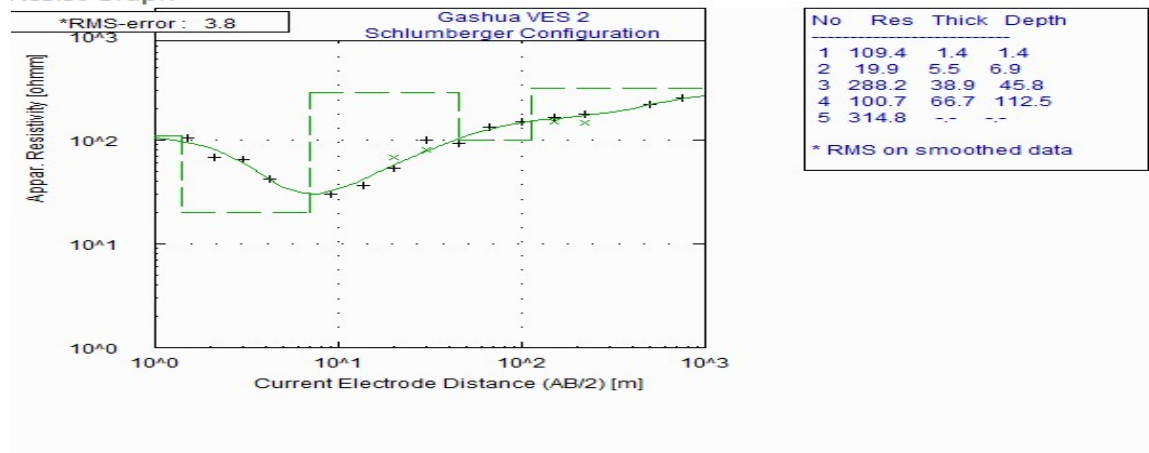
**APPENDIX**

**Vertical Electrical Resistivity Sounding Graphs.**

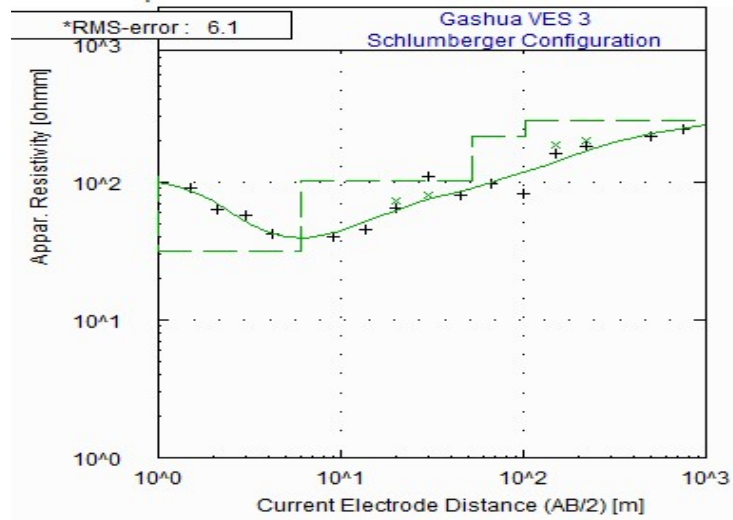
Resist Graph



Resist Graph



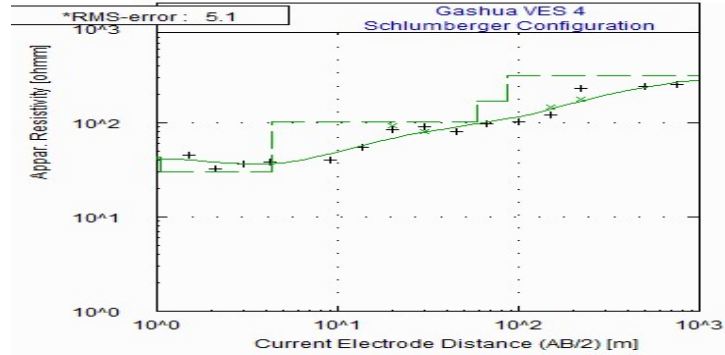
Resist Graph



No	Res	Thick	Depth
1	111.3	1.0	1.0
2	31.7	5.0	6.0
3	101.2	46.5	52.5
4	214.3	49.0	101.5
5	281.4	--	--

**\* RMS on smoothed data**

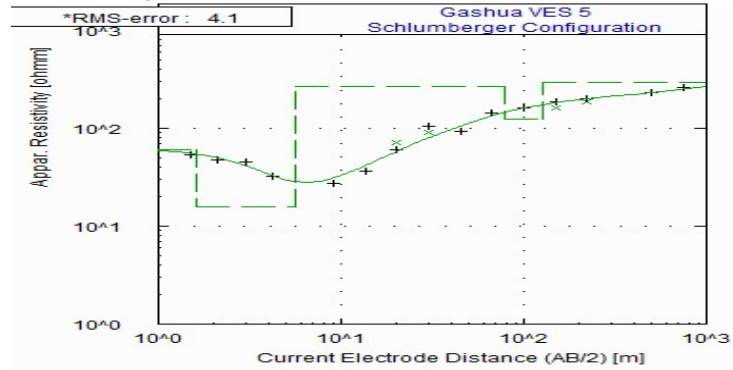
Resist Graph



No	Res	Thick	Depth
1	42.7	1.1	1.1
2	30.1	3.3	4.3
3	101.4	54.2	58.6
4	171.4	28.5	87.1
5	318.7	--	--

**\* RMS on smoothed data**

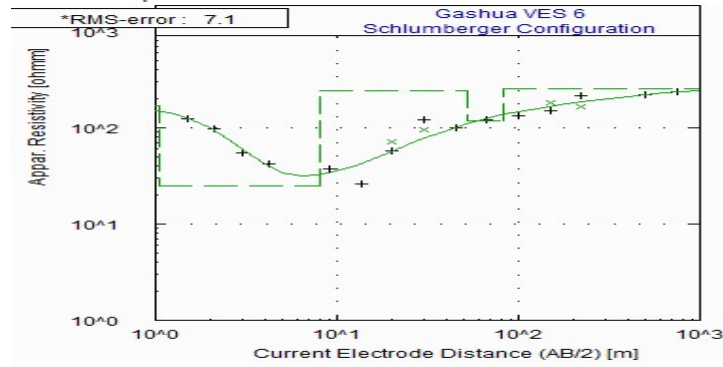
Resist Graph



No	Res	Thick	Depth
1	59.9	1.6	1.6
2	15.9	4.1	5.7
3	266.9	73.4	79.1
4	125.3	47.5	126.6
5	291.8	--	--

**\* RMS on smoothed data**

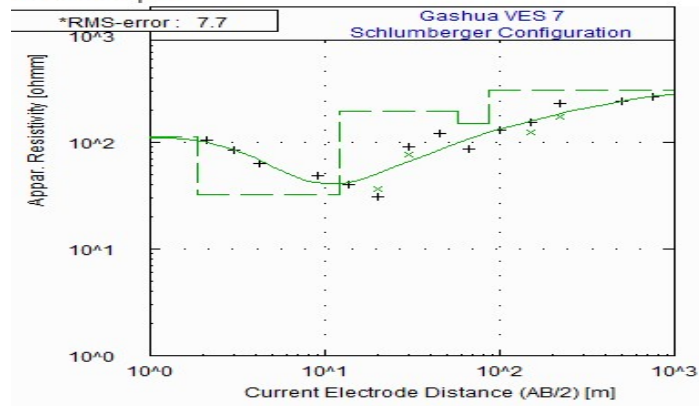
Resist Graph



No	Res	Thick	Depth
1	169.3	1.1	1.1
2	25.1	7.0	8.0
3	242.0	44.1	52.1
4	118.1	30.5	82.6
5	253.8	--	--

\* RMS on smoothed data

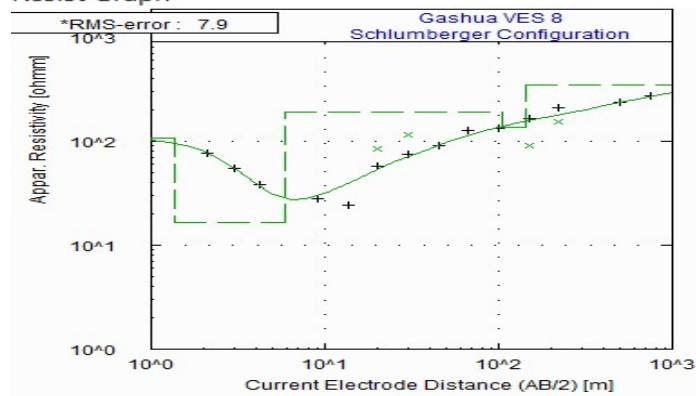
Resist Graph



No	Res	Thick	Depth
1	113.3	1.9	1.9
2	32.4	10.3	12.2
3	194.8	45.6	57.8
4	149.7	29.5	87.3
5	306.3	--	--

\* RMS on smoothed data

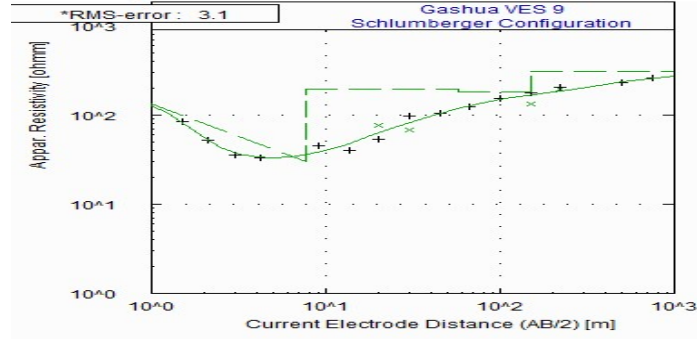
Resist Graph



No	Res	Thick	Depth
1	107.5	1.4	1.4
2	16.5	4.5	5.9
3	189.7	99.7	105.6
4	136.5	37.6	143.2
5	350.1	--	--

\* RMS on smoothed data

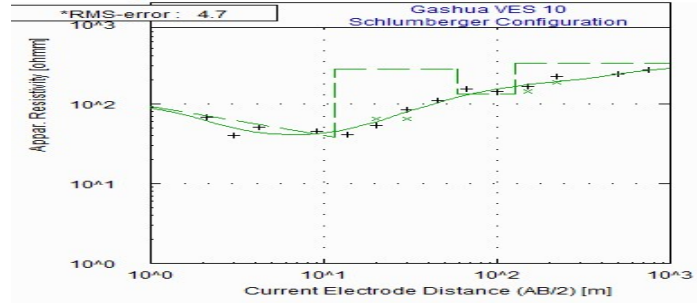
Resist Graph



No	Res	Thick	Depth
1	189.3	0.6	0.6
2	29.9	7.0	7.6
3	196.0	50.5	58.1
4	184.1	94.0	152.1
5	307.4	--	--

\* RMS on smoothed data

Resist Graph



No	Res	Thick	Depth
1	99.7	0.8	0.8
2	37.9	10.7	11.5
3	274.1	46.9	58.4
4	132.8	69.4	127.8
5	326.8	--	--

\* RMS on smoothed data

© GSJ